Low-Complexity Realization of a Concatenated DMT–FMT Multiuser Uplink System With Transmit Diversity

Andrea M. Tonello, *Member, IEEE*, and
Marco Bellin, *Student Member, IEEE*

***Abstract*—We present an efficient realization of a novel wireless uplink transmission scheme. The scheme concatenates an inner filtered multitone (FMT) modulator with transmission over multiple antennas and an outer space-time cyclically prefixed discrete multitone (DMT) modulator. The inner modulator is used to realize frequency-division multiplexing of the users by partitioning the FMT subchannels among them. The outer modulator copes with the residual subchannel intersymbol interference, and it further implements a form of transmit diversity. Frequency and space diversity is exploited via direct-sequence data spreading across the DMT tones. We also propose a multiuser analysis filter bank that significantly lowers the receiver complexity.**

***Index Terms*—Discrete multitone (DMT) modulation, filtered multitone (FMT) modulation, multiuser multiple-input–multiple-output (MIMO) systems, orthogonal frequency-division multiple access (OFDM), wireless uplink.**

I. Introduction

In this paper, we consider a recently presented air interface for the asynchronous multiple-access channel (uplink) based on the concatenation of multitone modulators [1]. It is intended for application in uplink wireless channels where the terminals experience frequency-selective fading, propagation delays, carrier-frequency offsets, and Doppler from movement, e.g., for fourth-generation cellular systems and for vehicle-to-vehicle or vehicle-to-infrastructure communications. These impairments may translate into multiple-access interference (MAI) that severely affects performance. The concatenated air interface combines an inner filtered multitone (FMT) modulator with an outer cyclically prefixed discrete multitone (DMT) modulator with multiple-antenna transmission. DMT is also known as orthogonal frequency-division multiplexing (OFDM). The inner modulator is used to efficiently realize frequency-division multiplexing by partitioning the FMT subchannels among the users. Differently from [2], where the FMT multiuser system adds a subchannel cyclic prefix (CP) to allow the use of subchannel frequency-domain equalization, we deploy the outer DMT modulator to cope with the residual intersymbol interference (ISI) of the FMT subchannels and to provide a form of transmit diversity referred to as cyclic delay diversity (CDD) in [3], [4]. It is referred to here as space-time cyclically prefixed DMT (ST-CP-DMT). Frequency and space diversity is exploited via direct-sequence (DS) data spreading. A detailed description of the scheme can be found in [1], and it is summarized here in Section II.

The key contribution of this paper is the efficient implementation of the DMT–FMT architecture that, as it will be shown, allows a significant complexity reduction, making the system more attractive for a real hardware realization. We show that the transmitter can be implemented via a concatenation of inverse discrete Fourier transforms (IDFTs) and low-rate polyphase filter banks. With reference to the receiver, first, we describe an efficient structure for the single-user receiver that is time and frequency synchronized to a given user (Section III). Then, we propose a novel low-complexity multiuser FMT analysis filter bank that allows the simultaneous detection of all subchannels of the asynchronous users (Section IV). We report a study of the complexity of the schemes herein described (Section V). Finally, we show that the multiuser architecture herein proposed yields performance close to the single-user case, but it exhibits a remarkable improvement in the multiuser case (Section VI).

Manuscript received February 29, 2008; revised July 29, 2008 and November 14, 2008. First published February 2, 2009; current version published August 14, 2009. This work was supported in part by the European Community's Seventh Framework Programme under Grant 213311, Project Omega—Home Gigabit Networks. This paper was presented in part at the 10th International Symposium on Spread Spectrum Techniques and Applications, Bologna, Italy, August 25–28, 2008. The review of this paper was coordinated by Dr. C. Yuen.

The authors are with the Dipartimento di Ingegneria Elettrica, Gestionale e Meccanica, Università di Udine, 33100 Udine, Italy (e-mail: tonello@uniud.it; marco.bellin@uniud.it).

Digital Object Identifier 10.1109/TVT.2009.2014382

II. Concatenated DMT–FMT Scheme

The users are multiplexed in a frequency-division fashion. The transmitter of each user (Fig. 1) comprises three stages: the DS data-spreading stage, the cyclically prefixed DMT modulation stage, and inner (with respect to the physical media) FMT modulation stage with transmission over N_T antennas. The spectrum is split by the FMT modulator into M slices that are assigned to distinct users. The antenna signals of a given user are simultaneously transmitted and occupy the spectrum corresponding to the assigned FMT subchannels. Each FMT subchannel is shaped with a prototype pulse having a frequency-concentrated response. With ideal band-limited pulses, the presence of time misalignments across users or channel time dispersion does not compromise the orthogonality between the users' signals. A frequency guard can be set to enhance the frequency separation of the FMT subchannels, which yields protection against the carrier-frequency offsets that may exist between users, although at the expense of the data rate [5]. The outer cyclically prefixed DMT modulator uses M_2 tones, and it is serially applied on each FMT subchannel to cope with the residual ISI that may arise because the FMT subchannels do not exhibit a perfectly flat frequency response.

The low-rate users that are assigned with a small number of FMT subchannels do not take advantage of the full frequency diversity that is provided by the broadband fading channel. In this case, the use of transmit diversity with multiple antennas is an effective means to increase performance. The ST-CP-DMT modulator is serially applied over each FMT subchannel, and it sends cyclically shifted replicas of the data blocks over the antennas [1], [3], [4]. It orthogonalizes the N_T spatial channels for any number of transmit antennas without decreasing the transmission rate. This allows the use of a conventional DMT receiver based on discrete Fourier transform (DFT). To exploit space and frequency diversity, we use DS data spreading across the DMT tones that fall within the FMT subchannels that are assigned to a given user. DS spreading does not decrease the transmission rate. The detection complexity is small using a zero-forcing or minimum-mean-square-error (MMSE) approach as it is herein considered [1], [6]. Furthermore, channel coding can also be added.

A. Transmitted Signal

The transmitted signal of user u and antenna t can be written as follows:

$$x^{(u,t)}(nT) = \sum_{k\in K_u} x^{(u,k,t)}(nT) = \sum_{k\in K_u}\sum_{\ell\in\mathbb{Z}} c^{(u,k,t)}(\ell T_0)\, g(nT-\ell T_0)\, e^{j2\pi f_k nT} \quad (1)$$

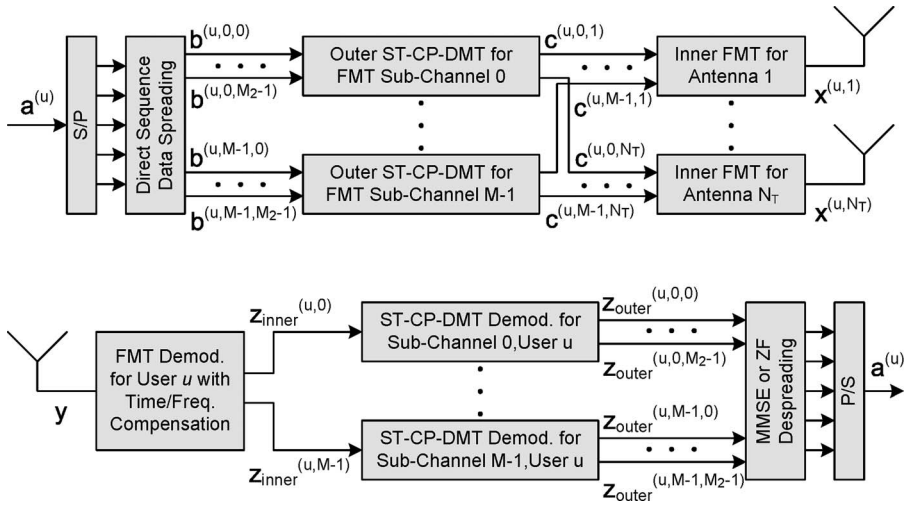

Fig. 1. Transmitter and single-user receiver for the concatenated scheme.

where $K_u \subseteq \{0,\dots,M-1\}$ is the set of tone indices assigned to user u, M is the number of FMT subchannels, T is the sampling period, $f_k = k/(MT)$ is the kth FMT carrier, $T_0 = NT$ is the FMT subchannel symbol period for a given integer $N \geq M$, $g(nT)$ is the prototype pulse with Nyquist band $1/2T_0$ (identical for all FMT subchannels), and $c^{(u,k,t)}(\ell T_0)$ is the sequence of symbols transmitted by user u over the FMT subchannel k and antenna t with period T_0. This sequence is obtained by an outer ST-CP-DMT modulator as follows. A block of M_2 symbols from the DS data-spreading stage is transformed by an M_2-point IDFT, and successively, a CP of length $\mu \geq 0$ is added to generate an output block of N_2 symbols to cope with the channel time dispersion due to frequency selectivity. The block, which has transmission period $T_2 = N_2 T_0$ with $N_2 = M_2 + \mu$, is passed to the FMT stage after the insertion of a cyclic delay. In formulas, we generate N_T blocks of N_2 symbols each as follows:

$$\begin{aligned} c^{(u,k,t)}(\ell T_0) &= c^{(u,k,t)}((n+mN_2)T_0) \\ &= \frac{1}{\sqrt{M_2 N_T}} \sum_{k'=0}^{M_2-1} b^{(u,k,k')}(mT_2) e^{j\frac{2\pi}{M_2}\left(n-\mu-\delta^{(t)}\right)k'} \end{aligned} \tag{2}$$

for $\ell = n + mN_2$, $n = 0,\dots,N_2-1$, $m \in \mathbb{Z}$, and $t = 1,\dots,N_T$. The parameter $\delta^{(t)}$ is the antenna t integer delay. It should be noted that the concatenation of the two modulators generates $L_u = M_u M_2$ narrow subchannels for user u, where $M_u \geq 1$ is the number of FMT subchannels that are assigned to user u.

According to (2), $b^{(u,k,k')}(mT_2)$ is the data symbol transmitted by user u over the DMT subchannel k' that falls within the FMT subchannel k, and it is obtained from the DS data-spreading stage to exploit frequency and spatial diversity [1]. We consider Walsh–Hadamard spreading of length L_u, although a shorter code can be used. Thus, starting from a block of L_u phase-shift keying (PSK)/quadrature-amplitude modulation (QAM) data symbols $a^{(u,i)}(mT_2)$, $i = 0,\dots,L_u-1$, of user u, spreading yields

$$b^{(u,k,k')}(mT_2) = \frac{1}{\sqrt{L_u}} \sum_{i=0}^{L_u-1} a^{(u,i)}(mT_2) s\left(i, k' + I^{(u)}(k) M_2\right) \tag{3}$$

where $k' = 0,\dots,M_2-1$, and $I^{(u)}(k) \in [0,\dots,M_u-1]$, for $k \in K_u$, is the inverse of the function that yields the indices of the FMT subchannels of user u. In (3), $s(i,n)$ are the elements of the Walsh–Hadamard matrix of size L_u. More details can be found in [1].

B. Single-User Detection Approach

The signals of the N_U users propagate through independent frequency-selective fading channels. We assume a discrete-time low-pass channel model and a single receiving antenna. Thus, the received sample at time instant $\tau_i = iT + \delta$ (where $i \in \mathbb{Z}$, and δ is a sampling phase) can be written as [5]

$$\begin{aligned} y(\tau_i) = \sum_{u=0}^{N_U-1} \sum_{t=1}^{N_T} \sum_{k\in K_u} \sum_{n\in\mathbb{Z}} x^{(u,k,t)}(nT) \\ \times g_{CH}^{(u,t)}\left(\tau_i - nT - \Delta_\tau^{(k)}\right) e^{j\left(2\pi\Delta_f^{(k)}\tau_i + \phi^{(k)}\right)} + w(\tau_i) \end{aligned} \tag{4}$$

where $w(\tau_i)$ is a sequence of independent identically distributed zero-mean complex Gaussian random variables, $g_{CH}^{(u,t)}(\tau)$ is the equivalent low-pass channel impulse response of the tth transmit antenna link of user u, and $\Delta_\tau^{(k)}$, $\Delta_f^{(k)}$, and $\phi^{(k)}$ are, respectively, the time offset, the carrier-frequency offset (assumed to be much smaller than $1/T$), and the phase offset of subchannel k. They are assumed identical for all antennas and subchannels assigned to a given user, i.e., $\Delta_\tau^{(k)} = \Delta_{\tau,u}$, $\Delta_f^{(k)} = \Delta_{f,u}$, and $\phi^{(k)} = \phi_u$, $\forall k \in K_u$.

As shown in Fig. 1, detection can be accomplished on a user-by-user basis with a three-stage receiver that first performs demodulation for the inner FMT modulator. That is, we first acquire time/frequency synchronization with each active user. Then, for each user, we run FMT demodulation via a bank of filters that is matched to the transmitter bank, and we sample the outputs at rate $1/T_0$. Successively, we run ST-CP-DMT demodulation, and finally, we apply MMSE despreading [6] and data decision.

III. Low Complexity Implementation

A. Efficient Synthesis Filter Bank With Concatenated ST-CP-DMT

An efficient implementation of the FMT synthesis stage is obtained by computing the polyphase decomposition [7] of (1) with period $T_3 = M_3 T$, assuming $M_3 = l.c.m.(M,N) = K_3 M = L_3 N$, where $l.c.m(\cdot,\cdot)$ is the least common multiple operator. The ith polyphase component reads

$$\begin{aligned} x^{(u,t,i)}(mT_3) &= x^{(u,t)}(iT + mT_3) \\ &= \sum_{\ell\in\mathbb{Z}} C^{(u,i,t)}(\ell T_0) g^{(i)}(mL_3T_0 - \ell T_0) \end{aligned} \tag{5}$$

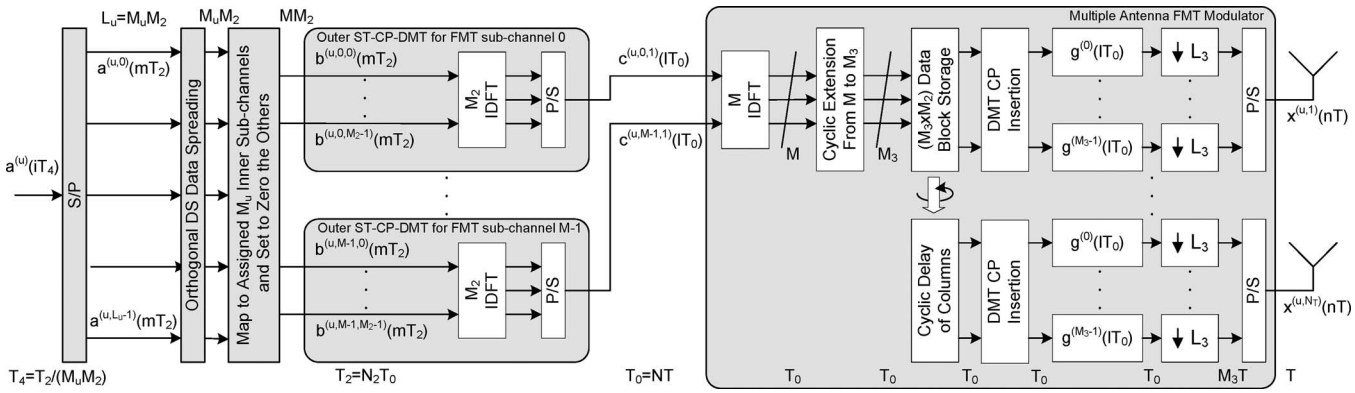

Fig. 2. Efficient realization of the ST-CP-DMT with FMT transmission for user u.

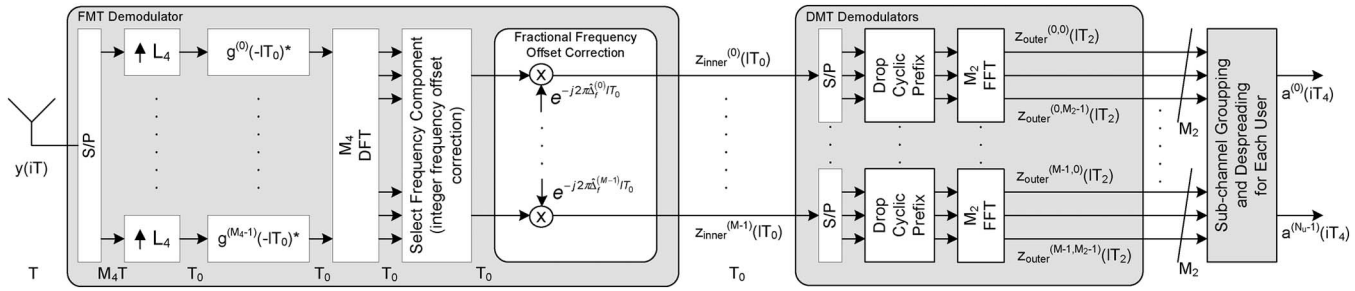

Fig. 3. Efficient realization of the multiuser receiver with a single filter bank.

for $i = 0, \ldots, M_3 - 1$ and $m \in \mathbb{Z}$, where the coefficients $C^{(u,i,t)}(\ell T_0) = \sum_{k=0}^{M-1} c^{(u,k,t)}(\ell T_0) e^{j(2\pi/M)ik}$ are obtained by the M-point IDFT of $\{c^{(u,k,t)}(\ell T_0)\}_{k=0,\ldots,M-1}$ followed by a cyclic extension with $M_3 - M$ elements. The cyclic extension corresponds to a K_3-time repetition of the block of M coefficients. The elements of $\{c^{(u,k,t)}(\ell T_0)\}_{k=0,\ldots,M-1}$ are zero for $k \notin K_u$. Furthermore, the ith polyphase component of the filter is

$$g^{(i)}(mL_3T_0 - \ell T_0) = g(iT + mT_3 - \ell T_0) \tag{6}$$

for $i = 0, \ldots, M_3 - 1$ and $m \in \mathbb{Z}$. It should be noted that differently from [8], the pulses here are time invariant.

Now, we can further simplify the scheme proposed in [1] since the sequences that feed the FMT modulators of the antennas with index $2 \div N_T$ are computed by taking the cyclic-delayed version of the sequence that feeds (before the CP insertion) the first modulator (Fig. 2). Therefore, the N_T FMT modulators can be implemented by using a single M-point IDFT, performing a cyclic extension from M to M_3, and storing the output coefficients. Then, we feed the various filter banks with the appropriate delayed version of the stored data blocks, and we add a prefix correspondent to the DMT CP.

B. Single-User Efficient Analysis Filter Bank

The analysis filter bank for the subchannels $k \in K_u$ of a given user u can be implemented via the polyphase decomposition of the received signal (4), after compensation of the time/frequency offset, i.e.,

$$y^{(u,i)}(\ell L_3 T_0) = y(iT + \ell L_3 T_0 + \Delta_{\tau,u}) e^{-j2\pi\Delta_{f,u}(iT + \ell L_3 T_0)} \tag{7}$$

for $i = 0, \ldots, M_3 - 1$. Then, the filter bank output for the subchannels of the desired user is obtained as follows:

$$z_{\text{inner}}^{(k)}(mT_0) = \sum_{i=0}^{M_3-1} Z^{(u,i)}(mT_0) e^{-j\frac{2\pi K_3}{M_3}ik} \tag{8}$$

$$Z^{(u,i)}(mT_0) = \sum_{\ell \in \mathbb{Z}} y^{(u,i)}(\ell L_3 T_0) g^{(i)}(\ell L_3 T_0 - mT_0)^*. \tag{9}$$

Note that the frequencies of the FMT subcarriers are $f_k = k/MT = K_3 k/M_3 T$, $k \in K_u$.

According to (8) and (9), the efficient realization comprises the following steps: compensation of the user time/frequency offset in the received signal, serial-to-parallel (S/P) conversion, interpolation by a factor L_3, filtering with the pulses $g^{(i)}(-mT_0)^*$, computation of an M_3-point DFT, and sampling the outputs at indices $K_3 k$, $k \in K_u$.

IV. Efficient Analysis Filter Bank for the Multiuser FMT Stage

Although the receiver filter bank is efficiently implemented according to the method described in Section III-B, it must be time and frequency synchronized to each user. In other words, we need to run one bank per user with time and frequency precompensation. Our goal is to devise a unique analysis filter bank that allows the detection of all users' signals (Fig. 3). We propose to use a common sampling phase δ for all the users. This has the effect of increasing the duration of the subchannel impulse responses since the users' signals have different time offsets. If such duration is shorter than the CP used by the DMT modulator, no ISI is experienced at the outer DMT demodulation stage output. Therefore, in the absence of frequency offsets, a single FMT filter bank would be enough to recover the users' signals. Unfortunately, uncompensated frequency offsets may cause interchannel interference (ICI), increased subchannel ISI, and constellation rotation (see, for instance, [1]). To jointly solve this problem and obtain an efficient architecture, we propose to compensate part of the frequency offsets before the filter bank and part after it, as explained in the following. In particular, we exploit the frequency resolution provided by the DFT.

First, we increase the frequency resolution of the structure presented in Section III-B, by defining $M_4 = QM_3 = K_4 M = L_4 N$, where Q is a positive integer, $K_4 = QK_3$, and $L_4 = QL_3$. Now, we can write

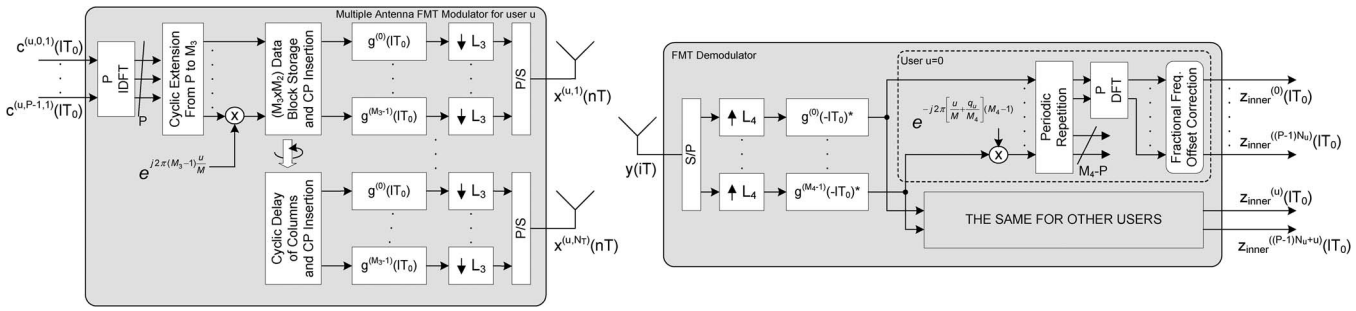

Fig. 4. Efficient architecture with interleaved-tone allocation.

the frequency offset as the sum of an integer part (multiple of the resolution $1/M_4T$) and a fractional part, i.e.,

$$\Delta_f^{(k)} = q^{(k)}/(M_4T) + \hat{\Delta}_f^{(k)}. \tag{10}$$

We assume that $|q^{(k)}| < \lfloor K_4/2 \rfloor$ for all k to avoid the complete overlapping of adjacent FMT subchannels ($\lfloor . \rfloor$ denotes the floor operation). Then, as a first step, we compensate only the integer part of the frequency offset. Thus, the kth FMT subchannel output can be written as

$$\begin{aligned} z_{\text{inner}}^{(k)}(mT_0) &= \sum_{i\in\mathbb{Z}} y(iT+\delta) e^{-j2\pi\left(f_k + \frac{q^{(k)}}{M_4T}\right)iT} g(iT - mT_0)^* \\ &= e^{j\left(2\pi\hat{\Delta}_f^{(k)} mT_0 + \varphi^{(k)}\right)} \sum_{t=1}^{N_T} \sum_{\ell\in\mathbb{Z}} c^{(u,k,t)}(\ell T_0) \\ &\quad \times g_{EQ}^{(u,k,t)}(mT_0 - \ell T_0) + \text{ICI}^{(k)}(mT_0) \\ &\quad + \text{MAI}^{(k)}(mT_0) + \eta^{(k)}(mT_0) \end{aligned} \tag{11}$$

that is, a useful signal term plus an ICI, MAI, and noise term, where $\varphi^{(k)} = 2\pi(f_k\delta - f_k\Delta_\tau^{(k)} + \Delta_f^{(k)}\delta) + \phi^{(k)}$. The ICI and MAI contributions are zero if we assume to use a perfectly frequency-confined prototype pulse with roll-off α_1 and all frequency offsets are smaller than the half of the guard band among subchannels, i.e., $\Delta_f^{(k)} < [N - M(1+\alpha_1)]/2MT_0$. Furthermore, the subchannel equivalent response reads

$$\begin{aligned} &g_{EQ}^{(u,k,t)}(mT_0 - \ell T_0) \\ &\quad = \sum_{i\in\mathbb{Z}} g_{CH}^{(u,t)}(iT) e^{-j2\pi f_k iT} \\ &\qquad \times \sum_{n\in\mathbb{Z}} g\left(nT - iT + mT_0 - \ell T_0 + \delta - \Delta_\tau^{(k)}\right) \\ &\qquad \times g(nT)^*\, e^{j2\pi\hat{\Delta}_f^{(k)} nT}. \end{aligned} \tag{12}$$

The modulation of the prototype pulse by $e^{j2\pi\hat{\Delta}_f^{(k)}nT}$ in (12) introduces an SNR loss and increased ISI. This is because the autocorrelation of the subchannel pulse is no longer a Nyquist pulse. The increased ISI can be, in principle, compensated by the outer CP-DMT stage (or by subchannel equalization [9]). If we assume that $\hat{\Delta}_f^{(k)}nT$ is approximately zero over the duration of $g(nT)$ (this is true for practical values of frequency offset), a further compensation of the rotation factor $e^{j2\pi\hat{\Delta}_f^{(k)}mT_0}$ in (11) fully corrects the frequency offset of the subchannel k. Note that this compensation is done at the subchannel level after the analysis stage.

The correction of the integer part of the frequency offset for all the users can be incorporated within the efficient implementation of the analysis filter bank, with no extra complexity. In fact, if we apply the polyphase decomposition to (11) with period M_4T, we obtain

$$z_{\text{inner}}^{(k)}(mT_0) = \sum_{i=0}^{M_4-1} Z^{(i)}(mT_0) e^{-j\frac{2\pi\left(K_4k+q^{(k)}\right)}{M_4}i} \tag{13}$$

$$Z^{(i)}(mT_0) = \sum_{\ell\in\mathbb{Z}} y^{(i)}(\ell L_4 T_0) g^{(i)}(\ell L_4 T_0 - mT_0)^* \tag{14}$$

$$y^{(i)}(\ell L_4 T_0) = y(iT + \ell L_4 T_0 + \delta), \qquad i = 0, \ldots, M_4 - 1.$$

According to (13) and (14), the realization in Fig. 3 is devised. It comprises the S/P conversion of the received signal, an interpolation by a factor L_4 of the subchannel signals, filtering with the prototype pulses $g^{(i)}(-mT_0)^*$, and the computation of an M_4-point DFT. To obtain the subchannel signals of user u and to partly compensate the frequency shift introduced by the carrier-frequency offset we choose the DFT outputs with index $K_4k + q^{(k)}$ for $k \in K_u$. Finally, we compensate the factor $e^{j2\pi\hat{\Delta}_f^{(k)}mT_0}$ at the DFT stage output.

If we assume to allocate the tones in an interleaved fashion, i.e., user u deploys the tones with index $kN_U + u$, $k = 0, \ldots, P-1$, and $P = M_u = M/N_U$, we can exploit the DFT properties similar to what has been done in [10] for an interleaved orthogonal frequency-division multiple-access system. The transmitter depicted in Fig. 2 can now be simplified by computing a P-point IDFT, followed by a cyclic extension with $M_3 - P$ coefficients and a phase rotation equal to $e^{j(2\pi iu/M)}$, $i = 0, \ldots, M_3 - 1$ (Fig. 4). At the receiver side, we can obtain the overall M subchannels deploying N_U P-point DFTs, instead of using an M_4-point DFT, as Fig. 4 shows. In fact, sampling the M_4-point DFT outputs in P regularly spaced points is equivalent to a modulation and a periodic transform of the input block followed by a P-point DFT. Moreover, we can include in the modulation the correction of the integer part of the frequency offset. The DFT associated to user u processes a block that is obtained by the M_4 coefficients at the output of the analysis stage, modulated by $e^{-j2\pi(u/M + q_u/M_4)i}$, $i = 0, \ldots, M_4 - 1$, and followed by a periodic transform of period P. The normalized integer carrier-frequency offset compensation q_u is chosen to be identical for all subchannels of user u, i.e., $q^{(k)} = q_u$ for every $k \in K_u$.

V. Complexity Analysis

To determine the savings in complexity w.r.t. the inefficient implementation and to benchmark the proposed scheme w.r.t. the conventional OFDM scheme, we evaluate the complexity in terms of the number of real operations per second. We assume that a complex multiplication requires six real operations, while a complex addition

requires two real operations. We further consider P interleaved tones per user.

First, at the transmitter, we have to take into account the complexity of DS data spreading and DMT modulation that is, respectively, equal to $[(PM_2-1)PM_2]/T_2$ and $(P\beta M_2 \log_2 M_2)/T_2$ operations per second per user, where β depends on the fast Fourier transform (FFT) algorithm. At the receiver, the complexity of DMT demodulation and despreading, respectively, equals $(P\beta M_2 \log_2 M_2)/T_2$ and $[(2PM_2-1)PM_2]/T_2$ real operations per second per user. It should be noted that this quantities remain unchanged with the number of antennas.

Second, we compute the complexity of the various FMT stage realizations. This is done below.

It should be noted that for a real implementation, other important parameters, e.g., the number of memory accesses, power consumption, and processing accuracy, should be taken into account. However, as, for instance, discussed in [11], such parameters depend on the DSP architecture and the specific processing procedures that implement the algorithms.

The complexity of the various FMT stage realizations is discussed in the following.

1) *Space-time FMT inefficient transmitter (IN-TX).* The conventional and inefficient realization of the transmitter in [1] comprises for every user N_T FMT inefficient modulators, each with P subchannels. Each subchannel has an interpolation filter with LN coefficients and one mixer. The outputs are then summed to yield

$$N_T \left[\underbrace{8PL-2P}_{\text{Filter Bank}} + \underbrace{6P}_{\text{Mixers}} + \underbrace{2(P-1)}_{\text{Subchannels Sum}} \right] /T \quad \text{[real op./s]}. \tag{15}$$

2) *Space-time FMT efficient transmitter (EF-TX).* This transmitter has been described in Section IV and depicted in Fig. 4. For each user, there is a unique P-point IDFT and M_3 multiplications for the modulation required by the interleaved-tone structure. Moreover, there are N_T filter banks, each one comprises M_3 decimator filters. The overall complexity is

$$\left[\underbrace{\beta P \log_2 P}_{\text{IFFT}} + \underbrace{6M_3}_{\text{Modulation}} + N_T \underbrace{(8NL-2N)}_{\text{Filter Bank}} \right] /T_0 \quad \text{[real op./s]}. \tag{16}$$

3) *FMT inefficient single-user receiver (SU-RX).* The conventional and inefficient realization of the single-user receiver in [1] comprises a frequency offset compensation block and a P-subchannel filter bank. Every subchannel has a decimation filter with LN coefficients and one mixer. Thus, the aggregate complexity for the N_U users is

$$N_U \left[\underbrace{6\text{N}}_{\text{Freq. Offset Corr.}} + \underbrace{6PN}_{\text{Mixers}} + \underbrace{P(8LN-2)}_{\text{Filter Bank}} \right] /T_0 \quad \text{[real op./s]}. \tag{17}$$

4) *FMT efficient multiuser analysis filter bank (MU-FB).* The structure of this receiver has been described in Section IV and depicted in Fig. 4. The unique analysis filter bank comprises M_4 interpolation filters. For each user, there is instead a P-point DFT, a postcorrection of the fractional frequency offset, and periodic repetition plus a modulation. The modulation is required by the interleaved-tone structure and comprises the correction of the integer part of the frequency offset. To compute the complexity of the periodic transform, we take into account the fact that only $\min(QM_3, LN)$ outputs of the filter bank differ from zero, and their position cyclically shifts in an *a priori* known fashion. Therefore, the complexity of the analysis filter bank is

$$N_U \left[\underbrace{K_4 P\,(8\lfloor L/L_4 \rfloor - 2)}_{\text{Filter Bank}} + \underbrace{8\min(QM_3, LN) - 2P}_{\text{Periodic Repetition and Modulation}} + \underbrace{\beta P \log_2 P}_{\text{FFT}} + \underbrace{6P}_{\text{Fractional. Freq. Offset Corr.}} \right] /T_0 \quad \text{[real op./s]}. \tag{18}$$

A. Numerical Results

A complexity comparison between the efficient and inefficient implementations is reported in Fig. 5. The numerical results are obtained by considering a system with 32 FMT subchannels interleaved among the users. The subchannel symbol period is $T_0 = NT = 40T$. The number of tones of the outer ST-CP-DMT modulator is $M_2 = 32$, and the CP length is $\mu = 8$. Thus, the aggregate symbol rate with FMT only is $R_{TOT-IN} = M/T_0 = 0.8/T$ symbols/s, while the aggregate rate with the outer modulator is $R_{TOT-OUT} = MM_2/(40T_0) = 0.64/T$ symbols/s. The prototype pulse is a finite-impulse-response root-raised cosine pulse with roll-off 0.2 and length LT_0, with L equal to 8 or 12. Moreover, we assume a Radix-2 FFT, and we use $\beta = 5$.

The curves show that the complexity savings with the proposed efficient implementations w.r.t. the inefficient one is significant. Clearly, reducing the pulse length decreases complexity. The multiuser analysis filter bank allows a high reduction in operations compared to the bank of inefficient single-user receivers. We also report the complexity of a baseline DMT (OFDM) system that uses CDD with $M_2M = 1024$ total tones as in the concatenated DMT–FMT scheme. Its complexity does not change with the number of transmit antennas. In particular, if we assume $N_U = 8$, $N_T = 1$, and $L = 8$, the complexity of the IN-TX is 328, while for the EF-TX and the DMT-TX, the complexity is, respectively, 137 and 10 real operations per unit time T per user. At the receiver side, the SU-RX and the MU-FB with parameter $Q = \{1, 4\}$ have, respectively, complexity equal to 336, 90, and 111 real operations per unit time T per user. The DMT-RX has complexity equal to 18 real operations per unit time T per user.

This shows that the baseline DMT system has lower complexity. The complexity increase in DMT–FMT is essentially due to subchannel filtering. However, the higher the number of users, the lower the difference between the complexity of the baseline DMT and the concatenated DMT–FMT scheme is.

We remark that in the plots, we do not consider the complexity due to data spreading and despreading, since the cost of these stages is identical for pure CDD DMT and concatenated DMT–FMT, assuming the same total number of DMT tones per user in both systems, as herein considered.

VI. Performance Comparisons

In Figs. 6 and 7, we report bit-error-rate (BER) performance assuming the same parameters in Section V-A. The users experience independent uniformly distributed time offsets in $[0, T_0]$ and carrier-frequency offsets in $[-\Delta_f^{\max}, \Delta_f^{\max}]$ that are assumed to be constant over the transmission of a frame of several outer DMT symbols. They deploy 4-PSK modulation and have equal average power. The channel is a T-spaced channel with an exponential power delay

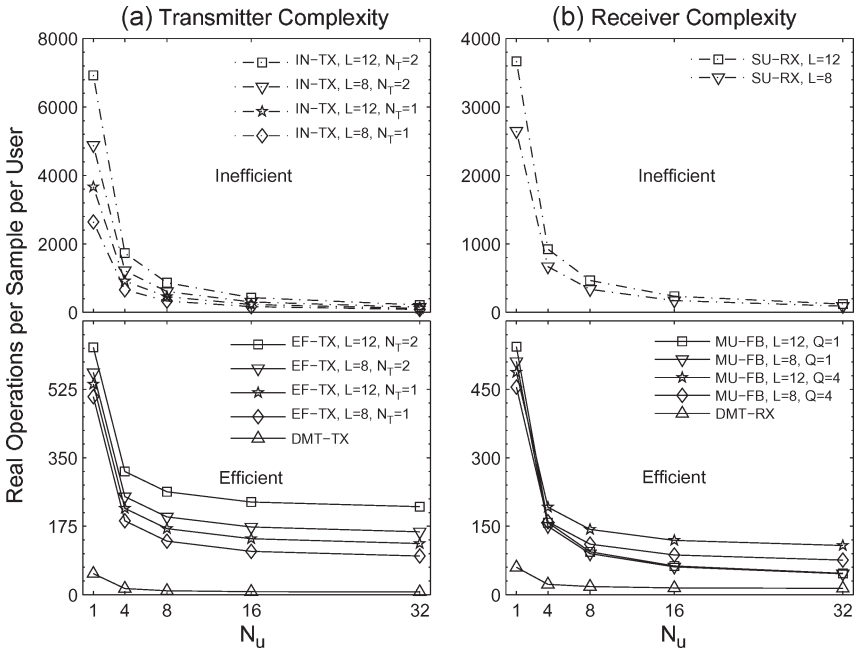

Fig. 5. Complexity comparison between DMT and concatenated DMT–FMT (efficient and inefficient implementations) for various numbers of transmit antennas, frequency resolution factors, and prototype pulse lengths. The complexity is computed in terms of real operations per second per user. (a) Transmitter. (b) Receiver.

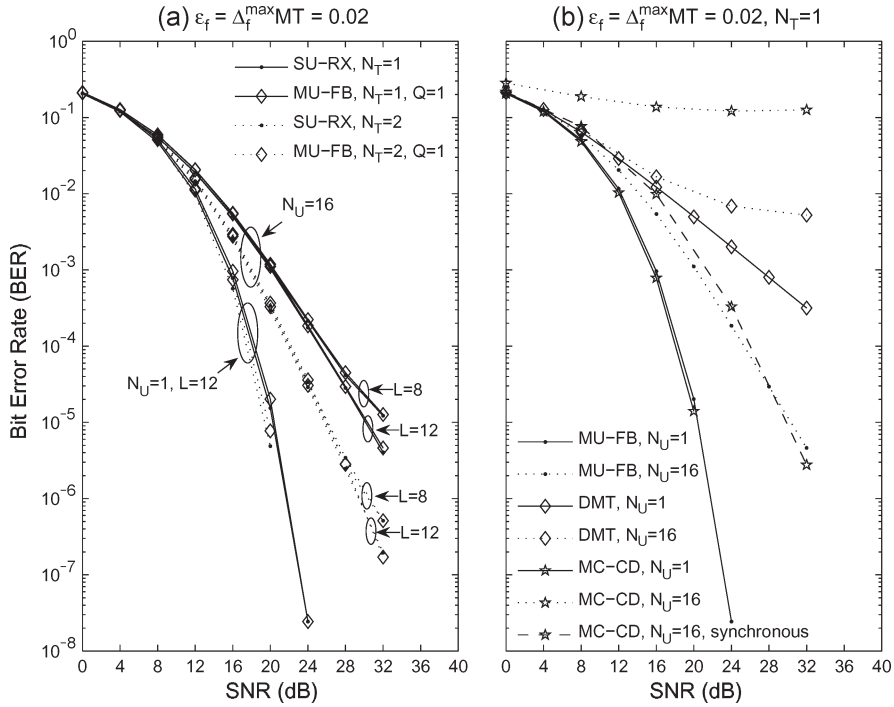

Fig. 6. (a) Average BER performance comparison between SU-RX and MU-FB for different numbers of users, different numbers of transmitting antennas, and different prototype pulse lengths LT_0 in a fully loaded system for a small-carrier-frequency-offset scenario. (b) Comparison between MU-FB, DMT, and MC-CDMA (MC-CD) for different numbers of users and one transmitting antenna for a small-carrier-frequency-offset scenario.

profile and independent Rayleigh-faded rays with average power $\Omega_p = e^{-pT/(\gamma T_0)}$, $p \in \mathbb{Z}$, for a normalized decay factor $\gamma = 0.2$ and truncation at -20 dB. The system is fully loaded (all subchannels are used), and the FMT tones are interleaved across the users. Perfect knowledge of the channel and time/frequency offsets is assumed. The cyclic delay for antenna t is set equal to $\delta^{(t)} = t - 1$. Spreading is accomplished with Walsh–Hadamard codes of length $L_u = M_2 M/N_U$ across the tones of the outer DMT modulator, e.g., $L_u = 1024$ with one user and $L_u = 32$ with 32 users. One-tap MMSE detection at the output of the ST-CP-DMT demodulator stage according to [1, eq. (20)] is used.

In Fig. 6(a), we plot the performance of the SU-RX and the MU-FB for $N_T = \{1, 2\}$ and $L = \{8, 12\}$ in a small-frequency-offset scenario, i.e., $\varepsilon_f = \Delta_f^{\max} MT = 0.02$ (the value is normalized to the subcarrier spacing). The proposed receiver performs close to the single-user receiver both with 1 and 16 users, which shows the robustness to the MAI. Marginal gains are found with $Q > 1$. Increasing the number of antennas to two yields significant gains with 16 users and only marginal gains with one user. With 16 users, decreasing the length of the prototype pulse yields a small error floor at high SNRs because we obtain a worse frequency confinement. However,

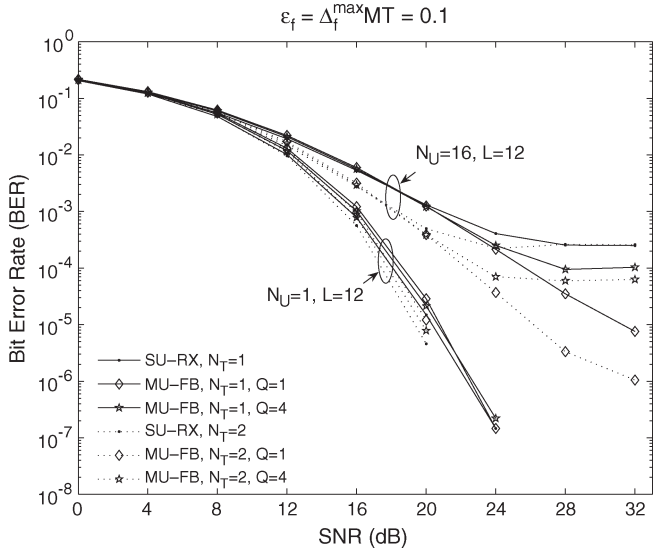

Fig. 7. Average BER performance comparison between SU-RX and MU-FB for different numbers of users and different numbers of transmitting antennas in a fully loaded system with a pulse of length $L = 12$ symbols for a large-carrier-frequency-offset scenario.

this reduces complexity, as discussed in Section V. For $N_U = 1$, we consider $L = 12$ only, since for $L = 8$, a negligible degradation of the performance has been found.

In Fig. 6(b), we also report the performance of a baseline DMT system and a multicarrier code-division multiple access (MC-CDMA) system, both with 1024 tones and a long CP of length 576 that is used for compensation of the user delays in excess of the channel duration. With these parameters, the three systems have the same aggregate transmission rate. The concatenated scheme with the simplified MU-FB receiver outperforms both DMT and MC-CDMA. MC-CDMA is severely affected by the uplink MAI, although to mitigate it, we deploy an MMSE multiuser detector [1], [6]. The users frequency offsets significantly worsen the BER of MC-CDMA.

The results with a large frequency offset are depicted in Fig. 7. Here, we set $\varepsilon_f = 0.1$ and $L = 12$. For $N_U = 1$, we can observe that the MU-FB achieves the performance of the single-user receiver by increasing the value of Q. This is due to the fact that with a larger frequency resolution, we are able to perform a fine precompensation of the frequency errors with a consequent increment of the energy that is collected by the matched filters. For $N_U = 16$, the MU-FB with $Q = 1$ yields a remarkable improvement compared to the single-user receiver. This is due to the fact that the SU-RX fully compensates the frequency offsets before the filter bank, which improves the useful signal energy, but it also increases the MAI contribution. On the contrary, with the MU-FB and $Q = 1$, we compute only a coarse frequency correction before the filter bank that yields a reduced MAI contribution. For $Q = 4$, we obtain an intermediate result.

VII. Conclusion

We have derived a computationally efficient architecture for the implementation of the recently proposed concatenated DMT with FMT and transmit diversity system. We have also proposed a low-complexity multiuser analysis filter bank that has robustness to channel frequency selectivity and users' time/frequency offsets. Furthermore, CDD with DS spreading allows obtaining diversity gains for the users that transmit at a low rate and occupy a fraction of the overall spectrum.

References

[1] A. Tonello, "A concatenated multitone multiple-antenna air-interface for the asynchronous multiple-access channel," *IEEE J. Sel. Areas Commun.—Special Issue on 4G Systems*, vol. 24, no. 3, pp. 457–469, Mar. 2006.

[2] G. Kang, M. Weckerle, and E. Costa, "Space-time joint channel estimation in filtered multi-tone based multi-carrier multi-branch system," in *Proc. WCNW*, Atlanta, GA, Mar. 21–25, 2004, pp. 1844–1849.

[3] A. Dammann and S. Kaiser, "Standard conformable antenna diversity techniques for OFDM and its application to the DVB-T system," in *Proc. IEEE Globecom*, Nov. 2001, pp. 3100–3105.

[4] G. Bauch and J. S. Malik, "Orthogonal frequency division multiple access with cyclic delay diversity," in *Proc. IEEE-ITG Workshop Smart Antennas*, Munich, Germany, Mar. 18–19, 2004, pp. 17–24.

[5] A. Tonello, "Asynchronous multicarrier multiple access: Optimal and sub-optimal detection and decoding," *Bell Labs Tech. J.*, vol. 7, no. 3, pp. 191–217, 2003.

[6] S. L. Miller and B. J. Rainbolt, "MMSE detection of multicarrier CDMA," *IEEE J. Sel. Areas Commun.*, vol. 18, no. 11, pp. 2356–2362, Nov. 2000.

[7] A. Tonello, "Time domain and frequency domain implementations of FMT modulation architectures," in *Proc. ICASSP*, Toulouse, France, May 2006, pp. 625–628.

[8] G. Cherubini, E. Eleftheriou, and S. Ölçer, "Filtered multitone modulation for very high-speed digital subscriber lines," *IEEE J. Sel. Areas Commun.*, vol. 20, no. 5, pp. 1016–1028, Jun. 2002.

[9] A. Tonello and M. Bellin, "An emerging concatenated multitone air interface for high speed access and home wireless networks," in *Proc. Globecom*, New Orleans, LA, Nov. 2008, pp. 1–5.

[10] A. Filippi and E. Costa, "Low-complexity interleaved subcarrier allocation in multicarrier multiple-access systems," *IEEE Trans. Commun.*, vol. 55, no. 1, pp. 35–39, Jan. 2007.

[11] N. Mizutani, S. Muramatsu, and H. Kikuchi, "Memory access estimation of filter bank implementation on different DSP architectures," *IEICE Trans. Fundam.*, vol. E84-A, no. 8, pp. 1951–1959, Aug. 2001.

Throughput-Based Switching Between Diversity and Multiplexing in MIMO Systems With Cochannel Interference

Jui Teng Wang

***Abstract*—A throughput-based switching scheme that uses the evaluated throughput as the criterion for switching between diversity and (spatial) multiplexing in multiple-input–multiple-output (MIMO) systems is proposed. The proposed throughput-based switching scheme can give a larger throughput than a MIMO scheme, with either diversity or multiplexing solely being employed. The joint beamforming and power control is further proposed for the throughput-based switching scheme to increase the received signal-to-interference-plus-noise ratio (SINR). With the increase in the received SINR, the throughput for the MIMO schemes [e.g., space-time block code (STBC) and Vertical Bell Laboratories Layered Space Time (V-BLAST)] can be further improved. We also show, through several properties, that the proposed joint beamforming and power control can increase the received SINR of each receive antenna so that the average SINR can converge to the target SINR, which, in turn, implies that the throughput can converge to the throughput requirement.**

***Index Terms*—Diversity, multiple-input–multiple-output (MIMO), multiplexing, space-time block code (STBC), Vertical Bell Laboratories Layered Space Time (V-BLAST).**

Manuscript received September 18, 2007; revised December 9, 2008. First published January 20, 2009; current version published August 14, 2009. The review of this paper was coordinated by Prof. S. Cui.

The author is with the Graduate Institute of Communication Engineering, National Chi Nan University, Puli, Nantou 545, Taiwan (e-mail: jtwang@ncnu.edu.tw).

Digital Object Identifier 10.1109/TVT.2009.2013355